Wide-Band Radiometry for Remote Sensing of Oil Films on Water

E. R. Brown, *Senior Member, IEEE,* O. B. McMahon, T. J. Murphy, *Member, IEEE,* G. G Hogan, G. D. Daniels, and G. Hover

***Abstract*— Total-power radiometry is applied over a wide-frequency band (26–40 GHz) to measure homogeneous and emulsified (40% : 60% oil : water composition) oil films on water. The resulting brightness-temperature (T_B) spectra contain substantially more information about the film than the spot-frequency measurements of previous work. In thin homogeneous films ($\sim$3 mm or less), the T_B spectra have the same monotonically increasing frequency dependence as the bare-water spectrum, but are distinguishable from the water by a positive T_B offset. For thicker homogeneous films, oscillations in the T_B spectra occur that have a period inversely related to the thickness of the film. For emulsified films, the T_B offset is greater than that of a homogeneous film of the same thickness, and oscillations in T_B occur, even for the thinnest (1 mm) emulsion tested. However, the amplitude of these oscillations is much smaller than for homogeneous films because of losses in the emulsion. Hence, the key result of this paper is that wide-band radiometry enables both the unambiguous determination of the thickness of homogeneous oil and the discrimination of homogeneous oil from emulsified films, at least in the range of thickness $>$1 mm.**

***Index Terms*— Antenna temperature, brightness temperature, dielectric constant of water, emissivity, Kirchoff's law, millimeter waves, oil films, radiometry, sky temperature, wide-band temperature.**

I. Introduction

MODERN electronics makes it possible to construct passive microwave or millimeter-wave receivers having an RF bandwidth that is a substantial fraction of the center operating frequency. These so-called wide-band receivers are very useful in short-pulse radar, electronic warfare, and certain other coherent applications. However, they can also be useful in environmental science, plasma physics, and other applications in which incoherent radiation must be transmitted or received over a broad frequency range. In such applications, passive radiometric receivers offer certain advantages over alternative active techniques, such as radar or reflectometry. Since a radiometer does not depend on strong retroreflection, it can measure an oil film over a large range of angles relative to the nadir. In addition, it does not suffer from speckle and other effects often encountered in coherent radar. Also, in most cases, radiometers are much simpler and less expensive than active receivers since neither high-power or ultra-low-noise oscillators are required.

In this paper, we address the problem of detecting the presence of an oil film on a body of water. Microwave radiometry was first applied to the oil-detection problem in the early 1970's [1], [2]. In the ideal case of uniform homogeneous oil films, radiometers operating at a single fixed frequency were used to show that the brightness temperature T_B was an oscillating function of film thickness. This oscillating function was found to lie above the background (bare water) T_B under most conditions. This allowed a unique determination of the thickness up to a value corresponding to the first peak of the oscillatory function, which is directly related to the operating frequency. However, films having a thickness beyond the first peak could only be measured with ambiguity since there would be at least one thinner layer that would yield the same T_B. A partial solution to this problem was to introduce a second operating frequency, well separated from the first. However, even in this case, two or more different films exist that yield the same T_B at each of the two operating frequencies. Hence, another operating frequency has to be added.

A more serious limitation of single- or dual-frequency radiometry occurs with inhomogeneous oil, such as the emulsions that result from the weathering and mixing action of oil and water. It is known that emulsified oil, like homogeneous oil, yields an increase in T_B above the water background [1]. Hence, at one or two fixed frequency points, an emulsified film of a given thickness may be difficult to distinguish from homogeneous films or from emulsion films of different thickness. In this paper, we show that wide-band radiometry allows an emulsion to be distinguished from homogeneous oil and allows the thickness to be estimated in a rough way.

II. Phenomenology

The electromagnetic power emanating from a body of water into the air above it can be understood from simple principles of radiative transport. At microwave and millimeter-wave frequencies, the power can be described by the Rayleigh–Jeans law, such that the power spectrum per spatial mode emanating from the body of water is given by kT_B^W where k is the Boltzmann's constant and T_B^W is the brightness temperature of the bare water. Similarly, in the presence of a thin film of oil or emulsion on the surface of the water, the power spectrum emanating into the air above is given by kT_B^o. The difference

Manuscript received April 30, 1997; revised June 27, 1998.

E. R. Brown was with Lincoln Laboratory, Massachusetts Institute of Technology, Lexington, MA 02173-9108 USA. He is now with the Electrical Engineering Department, University of California at Los Angeles, Los Angeles, CA 90095-1594 USA.

O. B. McMahon, T. J. Murphy, G. G Hogan, and G. D. Daniels are with Lincoln Laboratory, Massachusetts Institute of Technology, Lexington, MA 02173-9108 USA.

G. Hover is with the U.S. Coast Guard R&D Center, Marine Operations Technology Division, Groton, CT 06340-6096 USA.

Publisher Item Identifier S 0018-9480(98)09057-7.

between these two brightness temperatures is a metric for the observability of an oil film in experiments since T_B^W is usually the background against which measurements are made. Using Kirchoff's relation [3] and energy conservation, one can derive

$$T_B^o - T_B^W = (e_o - e_W)(T_W - T_B^s) \tag{1}$$

where e_W is the emissivity of the body of water, e_o is the emissivity of the oil film on the water, T_W is the physical temperature of the water, and T_B^s is the brightness temperature of the sky. T_W is practically constant in a given experimental setting, and T_B^s varies with frequency, but is generally much smaller in magnitude than T_W. Hence, (1) indicates that the difference in emissivities is an intrinsic driving factor for the measurable effect of different oil films on water.

One can calculate e_o and e_W using the optical theory of propagation through thin films. The analysis is particularly simple when the films are uniform in thickness, as the optical properties can then be calculated by matrix methods [4]. The radiation is assumed to propagate through the films as a plane wave at an angle of incidence of θ_A and the incident electric field polarized either vertical (V or TM) or horizontal (H or TE) relative to the plane of incidence. The reflection and refraction at each interface are assumed to be consistent with the Fresnel equations and Snell's law, with the polarization preserved throughout the medium. The important material parameters are the complex dielectric constants of oil ε_o and water ε_W. For the oil, the dielectric constant is assumed to be real ($\varepsilon_o = 2.0$), ignoring the small imaginary part that is usually less than 1% of the real part [5]. For the water, we assume a consistent dielectric constant given by the Debye model [6]

$$\varepsilon_W = \varepsilon_W^\infty + \frac{\varepsilon_W^0 - \varepsilon_W^\infty}{1 + i\omega\tau} \tag{2}$$

where ε_ω^0 is the static permittivity, $\varepsilon_\omega^\infty$ is the high-frequency permittivity, τ is the molecular relaxation time, and $i = \sqrt{-1}$. For the oil–water emulsion, the dielectric constant ε_E can be represented as a mixture according to an effective-media formulation [5]

$$\frac{\varepsilon_E - 1}{\varepsilon_E + 1} = \frac{\varepsilon_O - 1}{\varepsilon_O + 1} \cdot f_O + \frac{\varepsilon_W - 1}{\varepsilon_W + 1} \cdot f_W \tag{3}$$

where f_O and f_W are the oil and water fractions, respectively.

For example, fresh water has $\varepsilon_W^o = 80.0$ and $\varepsilon_W^\infty = 4.9$, and at a temperature of 10 °C has $\tau \approx 12$ ps [7]. Since ε_W^o is so large, the imaginary part of the dielectric constant is significant even at frequencies well above the inverse relaxation frequency $f = (2\pi\tau)^{-1} \approx 13$ GHz. At 33 GHz, for example, $\omega\tau = 2.49$ and $\varepsilon_W = 15.3 - 26.0i$. With the imaginary part this large, the reflectivity from the oil–water and air–water interfaces are rather high. For example, at 40° angle of incidence, Fresnel equations yield $R_{\mathrm{A/W}} = 0.62$ and $R_{\mathrm{O/W}} = 0.44$ for H polarization, and $R_{\mathrm{A/W}} = 0.44$ and $R_{\mathrm{O/W}} = 0.36$ for V polarization [8].

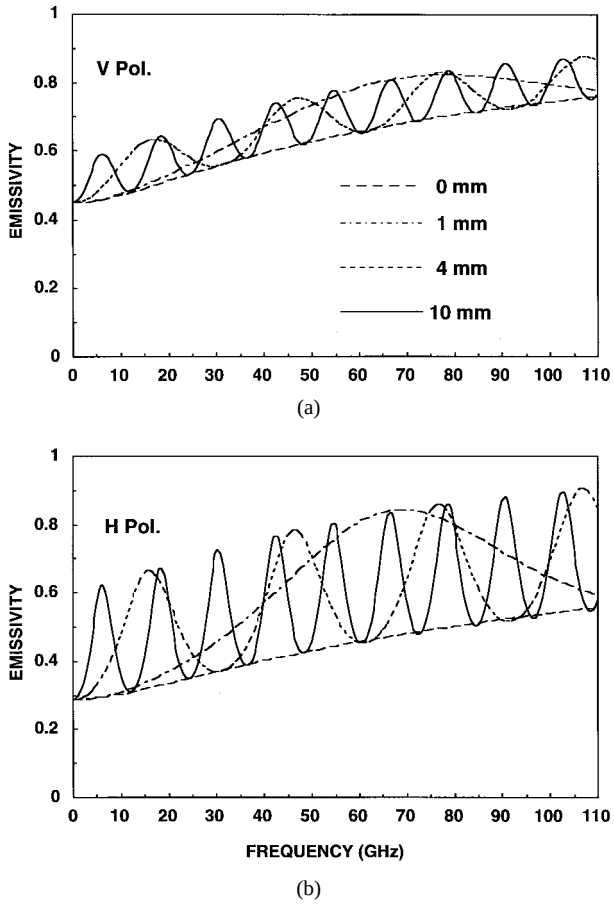

Fig. 1. (a) Theoretical emissivity versus frequency at 40° external angle for V polarization and oil-film thicknesses of 0, 1, 4, and 10 mm. (b) Emissivity versus frequency for same conditions as (a), except H polarization.

Using these dielectric models in the matrix formulation of propagation and assuming $\theta_A = 40°$ (the typical value in the present experiments), one obtains the emissivity curves of Fig. 1(a) and (b) for V and H polarization, respectively, from 0 to 110 GHz. Both plots are parametrized by the oil thickness for values of $d = 0$, 0.1, 0.4, and 1.0 cm, 1.0 cm being considered as roughly the greatest thickness encountered in practice. On inspecting these curves, several features stand out. First, oscillations occur versus frequency whose period is inversely related to the thickness. From the plane-wave analysis of the Appendix, the period is given by $\Delta f = c/\{2n_o d[1 - (\sin\theta_A/n_o)^2]^{1/2}\}$, where $n_o = (\varepsilon_o)^{1/2}$, θ_A is the angle of propagation in air, and d is the thickness of the film. The first peak occurs at $f_1 = \Delta f/2$, which yields 64.4, 16.1, and 6.4 GHz for 0.1, 0.4, and 1.0 cm, respectively. Other interesting features of Fig. 1 are: 1) the emissivity of water alone increases monotonically over the range, V lying above H polarization; 2) the emissivity with any oil present is greater than that of bare water; and 3) the amplitude of the oil-film emissivity oscillations is substantially greater for H than for V polarization. These features follow from the Debye model and Fresnel equations since the former dictates that the reflectivity of bare water will drop monotonically over the given range and the latter dictates that V polarization will have a lower reflectivity (particularly around Brewster's angle) than H polarization at all angles of incidence.

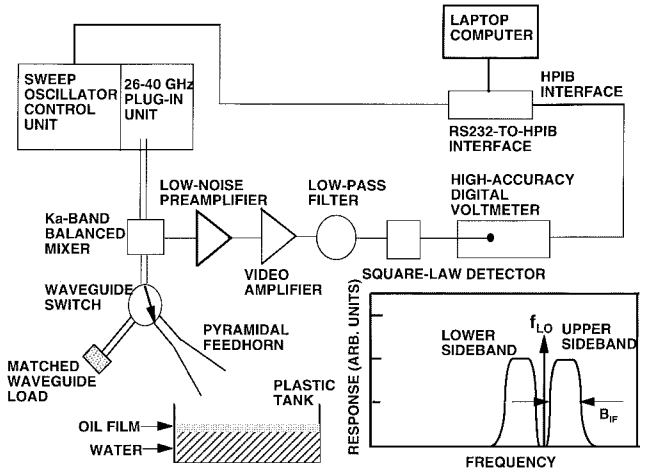

Fig. 2. Block diagram of FSR with double-sideband response and periodic gain normalization. The inset shows the double-sideband instrumental response.

TABLE I
FSR CHARACTERISTICS

Parameter	Ka Band	W Band
T_A (K)	171 (V), 125 (H)	229 (V), 190 (H)
T_M (K)	400	800
L (dB)	4	7
T_{IF} (K)	80	80
T_{SYS} (K)	771 (V), 725 (H)	1429 (V), 1390 (H)
B_{IF} (GHz)	0.5	0.5
τ (s)	0.1	0.1
$\Delta G/G$	0.00068	0.00068
ΔT (K)	0.54 (V), 0.50 (H)	0.99 (V), 0.96 (H)
d_{min} (mm)	0.34 (V), 0.25 (H)	0.25 (V), 0.17 (H)

III. FREQUENCY-STEPPING RADIOMETER

A. Radiometer Characteristics and Conditions

It is apparent from Fig. 1 that a relatively broad frequency range is required to measure a significant fraction of the period of the oscillating emissivity for even the thickest oil films. Hence, a prototype radiometer was developed to cover the entire range in Ka-band between 26 and 40 GHz, which was chosen for two reasons. Firstly, it is a band of relatively low atmospheric absorption, placed advantageously between the water absorption line at 22 GHz and the oxygen absorption complex at 60 GHz. Secondly, it represents a compromise between the superior sensitivity of front-end electronics at low frequencies (e.g., X-band) and the superior bandwidth (hence, superior oil-film thickness resolution) at higher (e.g., W-band) frequencies.

The radiometer was chosen as a traditional total-power heterodyne system with double-sideband frequency down-conversion and periodic gain normalization. A block diagram is shown in Fig. 2. The key front-end components are a frequency-tunable local oscillator (LO), a full-waveguide-band single-balanced mixer, and a low-noise preamplifier. The frequency-stepping radiometer (FSR) operates by mixing the input thermal radiation contained within the single spatial mode of the feedhorn with the LO signal to form a signal at the intermediate frequency (IF). At a given $f_{\rm LO}$, the parts of the Ka-band spectrum that are mixed down to the IF band lie within the ranges defined by $f_{\rm LO}+B_{\rm IF}$ (upper sideband) and $f_{\rm LO}-B_{\rm IF}$ (lower sideband), where $B_{\rm IF}$ is the electrical bandwidth of the electronic chain after the mixer. In this case, the IF bandwidth is defined by a bandpass characteristic associated with the turn-on frequency of the preamplifier f_1 ($\approx$1 MHz) and the corner frequency of a low-pass filter f_2. Since $f_1 \ll f_2$, $B_{\rm IF}$ is approximately equal to f_2.

The radiation collected by the FSR is determined by the pattern and orientation of the antenna, which was chosen to be a pyramidal Ka-band feedhorn. The pattern peaked at broadside with a full-width at the $-$10-dB points [$\Delta\Theta$(10 dB)] of approximately 30° in the E-plane and 22° in the H plane at 26 GHz. At 40 GHz, $\Delta\Theta(10\ \text{dB}) \approx 24°$ in the E-plane and 20° in the H plane. At both frequencies, the E-plane pattern contained small sidelobes.

Each of the experiments in this paper was conducted outdoors using a rectangular plastic tank and an open sky as the background. The tank was 24-in wide by 12-in long by 8-in deep, and was half filled with fresh water at the ambient temperature. In all cases, the feedhorn was oriented roughly 40° down from the nadir located approximately 18 in from the surface of the water at the center of the tank, and the E-plane of the feedhorn was aligned to the long dimension of the tank. Trigonometric calculations showed that the 10-dB footprint (including the E-plane sidelobes) was contained within the lateral extent of the tank, thus, the spillover was not a factor.

B. FSR Sensitivity

As in most other microwave and millimeter-wave radiometers, the sensitivity of the FSR is defined by a minimum detectable temperature difference ΔT [9] as follows:

$$\Delta T = T_{\rm sys}\sqrt{\frac{1}{B_{\rm IF}\tau_i}+\left(\frac{\Delta G}{G}\right)^2} \tag{4}$$

where $T_{\rm sys}$ is the system noise temperature, τ_i is the integration time, G is the overall electronic gain between the feedhorn and the square-law detector, and ΔG is the root mean square (rms) amplitude of the fluctuations in the gain over a time comparable to τ_i. $T_{\rm sys}$ accounts for electromagnetic noise that enters the receiver along with the signal to be measured, as well as electrical noise and transmission losses in the front end of the receiver itself. The predominant contributions are given by $T_{\rm sys} \equiv T_A + T_R \approx T_A + T_M + LT_{\rm IF}$ where T_R represents the noise power contributed by the receiver itself, T_M is the mixer noise temperature, L is its conversion loss, $T_{\rm IF}$ is the equivalent noise temperature of the IF electronics chain, and T_A is the antenna noise temperature, approximated here by the brightness temperature of the bare water T_B^W since this is the background against which the FSR must discriminate the presence of an oil film. Using the parameters listed in Table I and assuming $f = 33$ GHz and $\theta = 40°$, one finds

$T_R = 600$ K (double-sideband), $T_B^W = 171$ (V pol) and 125 K (H pol), and $T_{\rm sys} \approx 771$ (V pol) and 725 (H pol).

The primary contribution to ΔG is long-term $(>\tau_i)$ variations of $G_{\rm IF}$ caused by temperature-induced drift in the gain of the IF amplifiers. To mitigate this effect, the FSR was designed with temperature stabilization and periodic gain normalization. Nevertheless, some drift did occur, which by calibration was quantified as $\Delta G/G = 0.000\,68$. Substituting this into (4) along with $B_{\rm IF} = 0.5$ GHz and $\tau_i = 100$ ms, one finds $\Delta T = T_{\rm sys}(2 \times 10^{-8} + 4.6 \times 10^{-7})^{1/2}$, so that electronic-gain variations limit ΔT. Given the values of $T_{\rm sys}$ derived above, one then finds $\Delta T = 0.54$ K (V pol) and 0.50 K (H pol).

C. Operational Figures-of-Merit

Given the receiver sensitivity and radiative transfer characteristics discussed above, it is possible to derive figures-of-merit that characterize the capability of the FSR to measure thin oil. Two important figures are the minimum detectable thickness $d_{\rm min}$ and the measurable range of thickness Δd. Using the analytic approximations described in the Appendix, one finds the $d_{\rm min}$ given by (A.6). It depends on several FSR parameters, the most important being the operating wavelength, and the second most important being ΔT. For example, in the 26–40-GHz band, $T_B^s \approx 20+(10)/(14)(f-25)$ K. Then using $\lambda = 0.9$ cm, $n_0 = (2.0)^{1/2}$, $\theta_A = 40°$, the values of $R_{\rm A/W}$ and $R_{\rm O/W}$ defined in the Appendix, $T_W = 285$ K, and $\Delta T = 0.5$ K (as derived in Section III-B), one finds $d_{\rm min} = 0.34$ mm (V pol) and 0.25 mm (H pol).

A second important figure-of-merit is the range of thickness Δd, over which a measurement of T_B at any single frequency in the FSB band will be unambiguous. This can also be thought of as a range of thickness, starting at zero, over which T_B is greater than T_B^W by more than ΔT. For the simple case in the present FSR design of equally spaced frequencies, Δd can be determined by the Nyquist criterion. In the present context, the Nyquist criterion states that Δf must be equal to one-half the period of the oscillating T_B curve (i.e., the radiometer samples the sinusoidal term twice each cycle). Δd is then equal to the Nyquist thickness d_N, which is defined in the Appendix. For example, with $\Delta f = 1$ GHz, $n_0 = (2.0)^{1/2}$, and $\theta_A = 40°$, one finds $\Delta d = d_N \approx 6.0$ cm, which is greater than the thickest film typically encountered in unconfined oil spills.

IV. Experimental Results

To create the homogeneous films, crude oil was added to the tank with the specified thickness and allowed to settle for a few minutes, ensuring that air pockets were eliminated. For emulsions, a 40/60 mixture of oil and water was prepared with a blender and poured into the tank just prior to measurements. In all cases, the feedhorn was oriented in the manner described in Section III-A. To change polarization, a 90° twist was added to the Ka-band waveguide run just before the feedhorn, the hot–cold calibration was repeated, and the tank was rotated 90° about the nadir to keep the length of the tank along the E-plane of the horn.

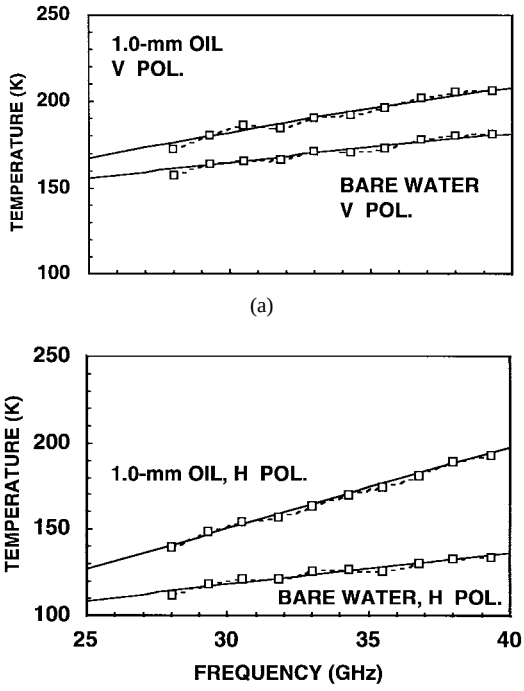

Fig. 3. Comparison of the experimental and theoretical T_B spectra for (a) V polarization. (b) H polarization emanating from bare water and a 1.0-mm oil film. The experimental points are denoted by open squares and are connected by a dashed line, while the theoretical curves are solid lines.

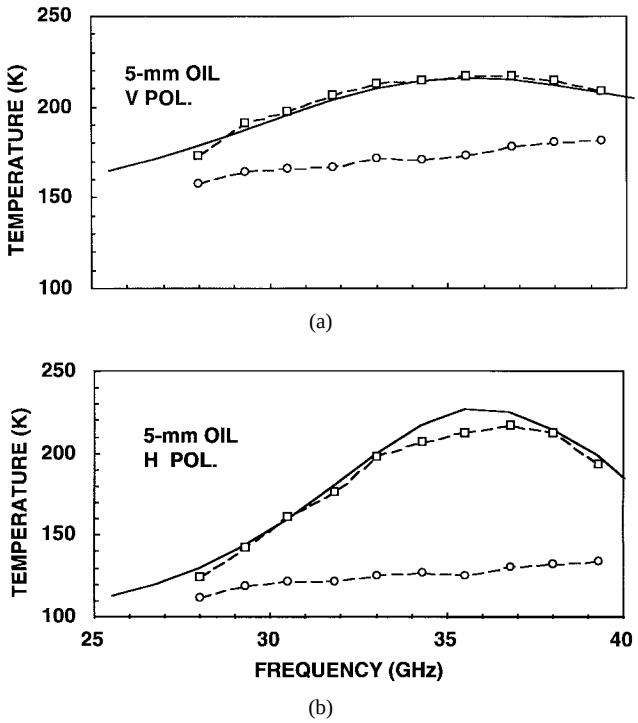

Fig. 4. Comparison of the experimental and theoretical T_B spectra for (a) V polarization, and (b) H polarization, emanating from a 5-mm oil film. The experimental points are denoted by open squares and are connected by a dashed line, while the theoretical curves are a solid line. The open circles represent the experimental date for bare water.

A. Homogeneous Oil Films

Several different uniform crude-oil layers were measured under a variety of sky conditions. Shown in Figs. 3 and 4

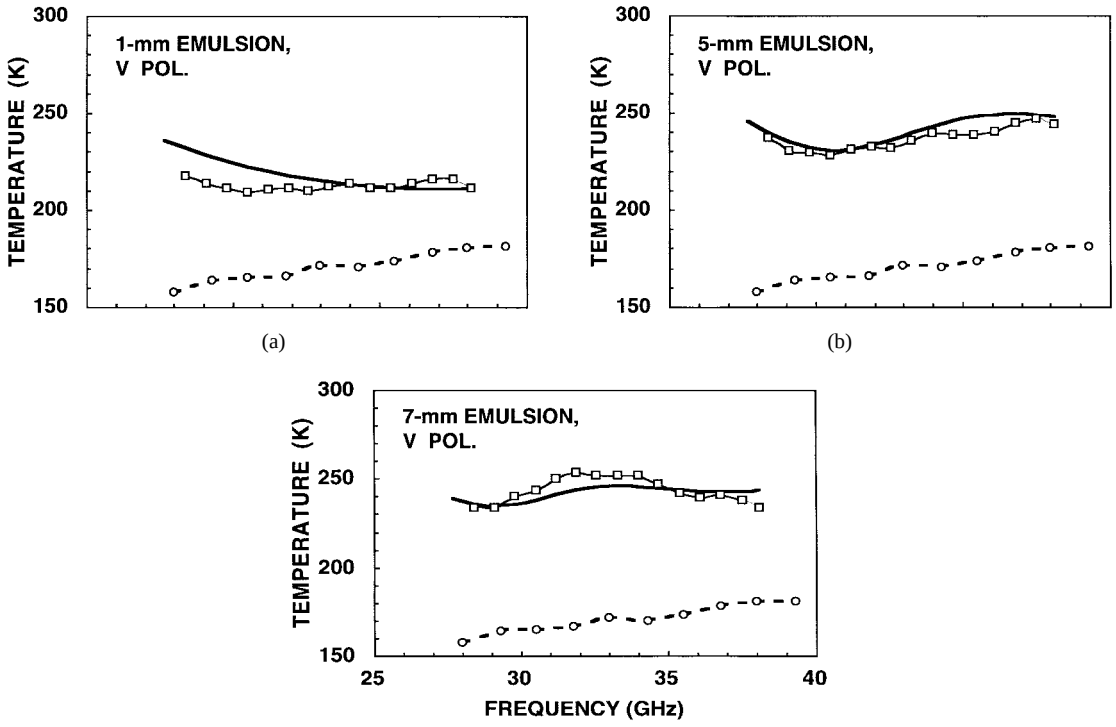

Fig. 5. Comparison of the experimental and theoretical T_B spectra for V-polarized radiation emanating from films of oil–water emulsion having thicknesses of (a) 1 mm, (b) 5 mm, and (c) 7 mm. In each case, the dashed line is the T_B spectrum for bare water.

are the experimental results for bare water and two films of thickness 1 and 5 mm. Superimposed on each plot is the corresponding curve of T_B computed from (1) and (2) and the assumptions that $T_W = 285$ K and that T_B^s varies linearly with frequency, as given in Section III-C. The bare-water experimental points for V and H polarization, plotted in Fig. 3(a) and (b), display the characteristics predicted in Section II. The T_B data for V polarization lies about 45 K above that for H polarization across the band. The data for both polarizations track the same gradual increase with frequency as the theoretical curve (solid line), and display a standard deviation δT from the theory (averaged over all data points) of 1.6 (V pol) and 1.0 K (H pol).

Superimposed in Fig. 3(a) and (b) are the T_B data points for V and H polarization taken on a film having a thickness of 1.0 mm. As predicted in Section II, H polarization yields nearly twice the offset between the oil-film spectrum and bare water as V polarization. As in the bare-water case, the experimental points track the theoretical curve, in this case, displaying a δT of 1.9 (V pol) and 1.0 K (H pol).

Shown in Fig. 4(a) and (b) are the T_B plots for the 5.0-mm film, which epitomize the advantage of wide-band radiometry. Unlike the spectra for bare water or thin films, the 5.0-mm film shows strong curvature associated with multiple-pass interference in the film. For V and H polarization, the data follows a concave-downward trend. At the T_B maxima around 36 GHz, the H-polarized data extends approximately twice as far above the bare-water level as the V-polarized data. The standard deviation δT between the experiment and theory is 2.6 (V pol) and 4.2 K (H pol). This deviation tends to grow with the thickness of the film.

B. Emulsions

Several different values of emulsion thickness were measured under the same conditions as the uniform films, except that only vertical polarization was applied. Plotted in Fig. 5 are the results for 1-, 5-, and 7-mm-thick oil. The first of these was the thinnest emulsion film studied in the present set of experiments. One distinguishing feature of the 1-mm spectrum is the large difference in T_B ($\approx$60 K) that occurs relative to bare water, compared to this difference for 1-mm-thick homogeneous oil ($\approx$15 K). A second feature is the nearly flat behavior versus frequency, compared to the upward slope for the 1-mm homogeneous film. This is attributed to the fact that the complex dielectric constant of the emulsion is much greater in modulus than the dielectric constant of the oil. Hence, even for the 1-mm emulsion, the first peak of the T_B curve occurs well below 26 GHz, so that downward behavior can be observed in Ka-band.

For the 5- and 7-mm-thick emulsion films, there is some additional upward offset compared to the 1-mm emulsion above 30 GHz. However, a more significant feature in both cases is curvature, which is concave up for the 5-mm film and concave down for the 7-mm film. Although somewhat surprising, the curvature was found to be repeatable. For the 7-mm film, it appears as though the spectrum is quasi-sinusoidal with one period roughly fitting across the 26–40-GHz band. The amplitude of the oscillation is 21 K, approximately half of the oscillation for thick homogenous films subject to V polarization.

Superimposed with each experimental curve is the theoretical curve of emulsion brightness temperature based on (1)

and (3). The agreement between experiment and theory is clearly inferior to that of homogeneous films. Nevertheless, the qualitative features of large dc offset relative to bare water and curvature for the thicker films are predicted by the theory. This lends confidence to the statement that emulsified films can be distinguished from homogeneous films by their substantially greater dc offset and their weaker curvature. This distinguishability is enabled by the wide-band operation of the radiometer. For example, in comparing the spectrum of the 1-mm emulsion film to that of the homogeneous 5-mm film of Fig. 5(a), the two spectra are clearly distinguishable by virtue of the downward curvature of the 5-mm film. However, if the two films were measured with a single-frequency radiometer operating at 33 GHz, T_B would measure approximately 212 K from both instruments, making the two films indistinguishable.

V. Higher Frequency Operation

Crude oil is a mixture of organic compounds (mostly heavy alkanes and aromatics) that have very little electromagnetic loss or dispersion in the microwave or millimeter-wave regions. As such, the amplitude of the T_B oscillations and the spacing between adjacent peaks changes little between dc and 110 GHz, as shown in Fig. 1(a) and (b). Hence, one expects on an intuitive level that the performance metrics for oil-film detection may improve by increasing the operating frequency. The main drawback of operating at frequencies above Ka-band is the increase in background sky temperature and the increase in the receiver noise that typically occurs. Above 40 GHz and for the assumed receive angle of 40°, the lowest value of T_B^s of approximately 80 K occurs at a local minimum in W-band [10].

To predict the FSR performance in W-band, we optimistically assume that 80 K is the value of T_B^s across the entire band and that $T_W = 285$ K, $\lambda = 0.33$ cm ($f = 91$ GHz), and $n_0 = (2.0)^{1/2}$, we can then use the Fresnel equations and (1) to write $R_W = 0.27$ and 0.47. Then, given the values in Table I, one finds $T_{\rm sys} = 1429$ and 1390 K, and $\Delta T = 0.99$ (V pol) and 0.96 K (H pol). The value of $d_{\rm min}$ is found by using these values along with $R_{\rm A/W} = R_W = 0.27$ (0.47) and $R_{\rm O/W} = 0.20$ (0.28) for V Pol (H Pol). Substituting these into (A.5), one finds $d_{\rm min} = 0.25$ (V pol) and 0.17 mm (H pol). This represents a 30% reduction in the $d_{\rm min}$ in spite of the substantial increase in $T_{\rm sys}$ that W-band operation entails.

VI. Summary

The primary goal of this paper was to demonstrate the benefits of wide-band total-power radiometry in the problem of measuring oil-bearing films on water. The main benefit is the uniqueness of the resulting T_B spectrum for each film. The distinguishing characteristic of the spectrum for thin homogeneous films ($\leq$3 mm) is a flat uniform offset from the spectrum of bare water, the magnitude of the offset scaling with the film thickness. Experiments on thin films of crude oil show that horizontal polarization yields nearly twice the offset of vertical polarization. A straightforward application of radiometric principles leads to the concept of a minimum detectable thickness, which for the present radiometer operating across Ka-band (26–40 GHz) is approximately 0.34 mm (V pol) and 0.25 mm (H pol).

The distinguishing feature of thicker homogeneous films (>3 mm) is oscillation in the spectrum with respect to frequency, the period of the T_B oscillations depending inversely on the thickness. Again, horizontal polarization yields a greater effect, having an oscillation amplitude of approximately 87 K, compared to 44 K for V polarization. Experiments and analysis on crude-oil show that the oscillations are quasi-sinusoidal, one period of the sinusoid falling within Ka-band for a thickness of 5 mm. For greater thickness, the period is reduced, but the amplitude remains roughly the same because of the weak absorption and dispersion in the oil at these frequencies.

The distinguishing feature of emulsions is a large offset (>50 K) above bare water, even for relatively thin films ($\sim$1 mm). The mean level of the T_B spectrum tends to remain roughly constant for emulsions thicker than this, but oscillations occur having an amplitude roughly half that of thick homogeneous films. Hence, a key conclusion of this paper is that emulsified films are distinguishable from homogeneous films by virtue of a spectrum having a large offset from bare water with small, but observable, oscillations. This is in contrast to the small offset with no oscillations for thin homogeneous films, and the large oscillations for thick homogeneous films.

Appendix
FSR Figures-of-Merit

A uniform homogeneous oil film on water is a special case that is very similar to the optical problem of a thin lossless dielectric film on a conducting substrate. Hence, we can apply the well-known optical result for transmission through such a film [4]

$$1 - R = T \approx \frac{(1-R_{\rm O/W})(1-R_{\rm O/A})}{1-2\sqrt{R_{\rm O/W}R_{\rm O/A}}\cos(2\delta+\phi)+R_{\rm O/W}R_{\rm O/A}} \tag{A.1}$$

where $R_{\rm O/W}$ and $R_{\rm O/A}$ are the power reflection coefficients at the oil–water and oil–air interfaces, respectively, ϕ is the phase change of the electric field upon reflection as the oil–water interface (radiation incident from the oil side), as defined by $r_{\rm O/W} = \sqrt{R_{\rm O/W}}\exp(i\phi)$, and δ is the optical phase difference between two successive transmitted rays, as given by $\delta = (2\pi d n_o/\lambda)\cos\theta_O = (2\pi d/\lambda)(n_O^2 - n_A^2\sin^2\theta_A)^{1/2}$, where the last step follows from Snell's law of refraction. In these expressions, n_O is the refractive index of the oil, d is the thickness of the film, λ is the wavelength of the radiation in vacuum, n_A is the refractive index of the air (nominally 1.0), and θ_A is the angle of propagation in the air relative to the normal direction.

A useful approximation to (A.1) results from the fact that the microwave refractive index of oil is low $[n_O \approx (2.0^{1/2}]$. This means that the field reflectivity for V polarization is

much less than unity when θ_A is near Brewster's angle or less ($\theta_B = \tan^{-1} n_o = 55°$), and the reflectivity for H polarization is much less than unity when θ_A is not too far from normal incidence. For example, at normal incidence Fresnel's equation yields $r_{\mathrm{O/A}} = (n_O - 1)/(n_O + 1) \approx 0.17$ (both states of polarization). A second useful approximation is based on the fact that up to about 100 GHz, the real part of the refractive index of water is much higher than that of oil. Hence, the phase shift upon reflection at the oil–water interface (radiation incident from the oil side) is close 180°, so that $\phi \approx \pi + \eta$ with $\eta \ll \pi$. This leads to $\cos(2\delta + \phi) = -\cos(2\delta + \eta)$. To take advantage of these approximations, we expand R in (A.1) to first order in $r_{\mathrm{O/A}} = (R_{\mathrm{O/A}})^{1/2}$

$$R_O \approx R_{\mathrm{O/W}} + 2\sqrt{R_{\mathrm{O/W}}}(1 - R_{\mathrm{O/W}}) r_{\mathrm{O/A}} \cos(2\delta + \eta). \tag{A.2}$$

In the limit of small values of δ and η, this reduces to $R_O \approx R_{\mathrm{O/W}} + 2\sqrt{R_{\mathrm{O/W}}}(1 - R_{\mathrm{O/W}}) r_{\mathrm{O/A}} \equiv R_{\mathrm{A/W}}$, a useful approximate expression for the reflectivity of the water–air interface. Note that $R_{\mathrm{A/W}}$ is greater than $R_{\mathrm{O/W}}$, as one should expect intuitively from the greater index contrast between air and water.

Upon substituting (A.2) into (A.1) and applying the variant of (1), $T_B^o = e_o T_W + R_o T_B^s$, we find

$$T_B^o - T_B^W \approx (R_{\mathrm{A/W}} - R_{\mathrm{O/W}}) \sin^2(\delta + \eta/2)(T_W - T_B^s) \tag{A.3}$$

and

$$e_o = e_W = (R_{\mathrm{A/W}} - R_{\mathrm{O/W}}) \sin^2(\delta + \eta/2) \tag{A.4}$$

where the identity $\cos 2\delta = 1 - 2\sin^2 \delta$ has been used.

Equation (A.3) is useful in establishing criteria related to the measurement of an arbitrary oil film by a passive radiometer. The first criterion of interest is the minimum oil-film thickness $d_{\min}$ that the radiometer can measure in the presence of noise. To estimate this, we assume that the noise contributions internal and external to the radiometer can be represented by the minimum detectable temperature ΔT, as discussed in Section III-B. We then take the bare water T_B as a baseline and substitute $T_B^W + \Delta T$ for T_B^o in (A.3). Solving for the thickness using the expression for δ, given after (A.1), and the definition of R_O, given after (A.2), we find the result

$$d_{\min} = \frac{\lambda}{2\pi\sqrt{n_o^2 - \sin^2\theta_A}} \cdot \left\{ \sin^{-1}\left[\sqrt{\frac{\Delta T}{(R_{\mathrm{A/W}} - R_{\mathrm{O/W}})(T_W - T_B^s)}} \right] - \frac{\eta}{2} \right\}. \tag{A.5}$$

The second criterion of interest is the range of thickness Δd, over which a measurement of T_B at any single frequency will be unambiguous. This can also be thought of as a range of thickness, starting at zero, over which T_B is greater than T_B^W by more than ΔT. We determine Δd by seeking the closest values of d, say, d_1 and d_2, in the $\sin^2$ argument of (A.3) that yield the same value of T_B. Since the $\sin^2$ function oscillates with period π, we can write $\pi = \delta_2 - \delta_1 = (d_2 - d_1)(2\pi n_o \cos\theta_o)/\lambda$ or $\Delta d = \lambda/(2n_o \cos\theta_o)$. Using Snell's law, we can recast this as $\Delta d = \lambda/2\sqrt{n_o^2 - \sin^2\theta_A}$. As an example, for $\lambda = 0.9$ cm, $n_0 = (2.0)^{1/2}$, and $\theta_A = 40°$, we find $\Delta d = 0.35$ cm. Although this range may seem prohibitively small, it could be extended simply by adding a measurement of T_B at a different frequency. Of course, there will still be a thickness, which, according to (A.3), yields the same value of T_B for any two distinct frequencies. As the two frequencies are moved closer together, the thickness of ambiguity rises. However, a new ambiguity effect enters when the T_B values for the closely spaced frequencies become less than or equal to ΔT. *This explains the motivation to measure a multitude of frequencies (i.e., more than two) in any radiometric determination of uniform films of oil on water*.

Perhaps the simplest multiple-frequency radiometric scheme is to measure T_B at values $f_1, f_2, \cdots, f_N$, which are equally spaced with separation Δf. The thickness range can then be determined by the Nyquist criterion. In the present context, the Nyquist criterion states that Δf must be equal to one-half the period of the oscillating T_B (i.e., the radiometer samples the $\sin^2$ term twice each cycle). Since $\sin^2\delta$ oscillates twice as fast as $\sin\delta$, Δf must correspond to the difference between $\delta = \pi/2 = 2\pi d_N n_0 \cos\theta_0 f/c$ and $\delta = 0$. The quantity d_N, called the Nyquist thickness by convention, is also equal to the unambiguous thickness range Δd defined above. Using Snell's law to recast $\cos\theta_0$, we find the relation (independent of polarization)

$$\Delta d = d_N = \frac{c}{4\Delta f\sqrt{n_0^2 - \sin^2\theta_A}}. \tag{A.6}$$

REFERENCES

[1] A. T. Edgerton and D. Trexler, "Radiometric detection of oil slicks," Aerojet General Corporation, El Monte, CA, Rep. SD1335-1, Jan. 1970.

[2] J. P. Hollinger and R. A. Manella, "Oil spills: Measurements of their distributions and volumes by multifrequency microwave radiometry," *Science*, vol. 181, pp. 54–56, 1973.

[3] J. B. Marion, *Classical Electromagnetic Radiation*. New York: Academic, 1965, secs. 6.5 and 11.10.

[4] M. Born and E. Wolf, *Principles of Optics*, 2nd ed. New York: Pergamon, 1975.

[5] N. Skou, *IEEE Trans. Geosci. Remote Sensing*, vol. GE-24, pp. 360–367, May 1981.

[6] P. Debye, *Polar Molecules*. New York: Dover, 1945.

[7] F. T. Ulaby, R. K. Moore, and A. K. Fung, *Microwave Remote Sensing: Active and Passive*, vol. III. Reading, MA: Addison-Wesley, 1981.

[8] J. D. Jackson, *Classical Electrodynamics*. New York: Wiley, 1975, sec. 7.3.

[9] A. F. Harvey, "Radiometric techniques," *Microwave Engineering*. New York: Academic, 1963, pp. 773–783.

[10] F. T. Ulaby, R. K. Moore, and A. K. Fung, *Microwave Remote Sensing: Active and Passive*, vol. III. Reading, MA: Addison-Wesley, 1981, pp. 283–286.

E. R. Brown (M'92–SM'97) received the B.S. degree in physics from the University of California at Los Angeles (UCLA), in 1979, and the Ph.D. and master's degrees in applied physics from the California Institute of Technology, Pasadena, in 1985 and 1981, respectively, where he conducted research on millimeter-wave and terahertz mixers made from semiconductor hot-electron bolometers and magnetically quantized photoconductors.

He is currently a Professor of electrical engineering at UCLA, and is a part-time Technical Staff Member at the Jet Propulsion Laboratory, Pasadena, CA. He is currently developing research projects in power electromagnetics, ultrafast electronics and optoelectronics, advanced RF sensor technology, and biomedical engineering. Prior to joining UCLA, he was a Program Manager at the Defense Advanced Research Projects Agency (DARPA Electronics Technology Office), Arlington, VA, where he helped create and manage programs in advanced RF technology (MAFET Thrust 3), high-power solid-state electronics (Megawatt), highly controlled infrared dielectric emissivity (HIDE), and advanced acoustics technology (Sonoelectronics). Each of these programs was aimed at revolutionary breakthroughs in device and component technology, and was tailored for system integration and transition of the successful technologies. For example, the MAFET Thrust-3 Program introduced several new device and circuit technologies, such as RF microelectromechanical (MEMS) switches and three-dimensional bulk-micromachined integrated circuits (IC's), which are already being transitioned to system programs. Prior to DARPA, he was an Assistant Group Leader and Staff Researcher at the MIT Lincoln Laboratory, Lexington, MA, where he conducted original research and development in advanced electromagnetics, ultrafast electronics and optoelectronics, solid-state device physics, and high-frequency receiver technology. Among his key inventions and discoveries were the photonic-crystal planar antenna, the low-temperature-grown-GaAs terahertz photomixer, the resonant-tunneling-diode relaxation oscillator, normal-incidence absorption in semiconductor quantum wells, and shot-noise suppression and quantum-transport inductance in resonant-tunneling devices. Each of these has been unique in terms of device performance or scientific contribution. For example, the photonic-crystal planar antenna was the first RF application that utilized the three-dimensional nature of the photonic stopbands, and has helped point towards a new direction in monolithic IC's, whereby the semiconductor substrate can be fabricated to improve rather than degrade the performance of passive RF components. From 1977 to 1981, he received fellowships at the Hughes Aircraft Company, where he worked on key components in millimeter-wave radiometers and high-speed ($>$1 Gbit/s) laser communications systems for the Space and Communications Group, El Segundo, CA.

Dr. Brown is a member of Phi Beta Kappa, the American Physical Society, and the Materials Research Society. He was the recipient of a 1998 Achievement Award presented by the Office of Secretary of Defense.

O. B. McMahon, photograph and biography not available at the time of publication.

T. J. Murphy, (S'78–M'78), photograph and biography not available at the time of publication.

G. G Hogan, photograph and biography not available at the time of publication.

G. D. Daniels, photograph and biography not available at the time of publication.

G. Hover, photograph and biography not available at the time of publication.